Eur. Phys. J. Plus (2022) 137:1105
https://doi.org/10.1140/epjp/s13360-022-03312-3

THE EUROPEAN PHYSICAL JOURNAL PLUS

Regular Article

Development of nanosized ZnO-PVA-based polymer composite films for performance efficiency optimisation of organic solar cells

Fazal Ur Rehman[1,2,3], **Manzar Zahra**[1], **Ali H. Reshak**[4,5,a], **Iqra Qayyum**[1,2], **Aoun Raza**[1], **Zeshan Zada**[6], **Shafqat Zada**[7], **Muhammad M. Ramli**[5]

[1] Department of Chemistry, Lahore Garrison University, Lahore, Pakistan
[2] Department of Chemistry, University of Education, Lahore, Pakistan
[3] Advance Analytical Development Lab-Research and Development Department, CCL Pharmaceuticals, Lahore 54000, Pakistan
[4] Physics Department, College of Science, University of Basrah, Basrah 61004, Iraq
[5] Center of Excellence Geopolymer and Green Technology (CEGeoGTech), University Malaysia Perlis, 01007 Kangar, Perlis, Malaysia
[6] Material Modelling Lab, Department of Physics, Islamia College Peshawar, Peshawar, KP, Pakistan
[7] Department of Biochemistry, Quaid-E-Azam University, Islamabad, Pakistan

Received: 26 July 2022 / Accepted: 21 September 2022

Abstract Due to flexibility, environmental-friendliness, lower temperature growth, solution tunability, and flexibility of addition, organic solar cells (OSCs) are increasingly attracting prominence in photovoltaics. Despite these benefits, OSCs have a lower energy conversion efficiency than conventional solar-powered cells. As a result, increasing OSC effectiveness will inevitably be the focus. Using this idea, we developed the ZnO-integrated PVA nanocomposite (NCs) films to determine whether we could enhance their effectiveness. The NCs films were made utilising the Solution Casting Approach with a variety of ZnO nanoparticle concentrations in a PVA matrix. Each NCs film sample was examined using OSCs. OSC effectiveness varies significantly with and without using developed NCs films. When used on OSCs with the structure [carbon fibre]/(CuO/epoxy resin)/(ZnO/epoxy resin)/carbon fibre, the film with the appropriate weight percent of ZnO, 16.50%, and PVA, 83.50%, demonstrates a noticeable improvement in performance efficiency.

Abbreviations

NPs	Nanoparticles
OSCs	Organic solar cells
NCs	Nanocomposites
PCMs	Polymer composite materials
PMs	Polymeric materials

1 Introduction

Nanotechnology has immense promise for successfully gathering solar energy using photovoltaic (PV) cells. When organic solar devices modified with different polymers and inorganic cells are modified by doping with silicon, nanosized particles (NPs) act as semiconductor in PV devices [1]. Polymer materials (PMs) are used to replace conventional materials as they are lightweight, affordable, and have significant physio-chemical properties [2]. Remarkable efforts have been done to develop the varied NCs in order to understand their basic rules in a variety of sustainable energy [3].

By adding minuscule amounts of nanofillers to polymer matrices, it is possible to modify the properties of PMs (such as their structural, optical, mechanical, and electrical properties) [4]. ZnO NPs are used in several applications, including photo-electronic devices and UV absorption, due to their unique properties. In order to measure the physical properties of PCMs, fundamental polymer matrix with doped ZnO NPs has proved to be very helpful [5]. These NPs appear to develop a compound with the polymeric chains, optimising the physio-chemical behaviours of polymeric composite materials (PCMs).

Polyvinyl alcohol (PVA) has recently been used as a basic polymer material with specific qualities like environmental stability, high stability, bio-degradability, electrical and optical capabilities. A fundamental aspect of PVA's semi-crystalline structure is

[a] e-mail: maalidph@yahoo.co.uk (corresponding author)

Published online: 04 October 2022

the coexistence of amorphous and crystalline zones, which develops concentric amorphous-crystal properties to increase physical qualities [6].

In the third-generation off solar devices, which were employed to build solution-coated OSCs, organic materials, particularly semiconducting polymeric polymers, were utilised as light absorbers [7]. PCMs, which have lower production costs and better performance, are principally required for third-generation OSCs. Third-generation OSCs, or thin film OSCs, are assembled with more and more NCs to enhance solar energy collecting [8]. The most crucial factors in establishing if a material is practical for using solar energy are its optical absorption, environmental stability, and conductivity.

Optoelectronics is seeing an increase in the use of PCMs. Due of their numerous uses, ZnO-based NCs have drawn the attention of several research scientists [9]. Mechanical, electrical, and optical properties of polymers can be altered by adding ZnO NPs to PVA frameworks. Polymer-based NCs are produced using a variety of procedures [10]. Each strategy has unique characteristics of its own. But regardless of strategy, ultimate morphology is the main focus of all PCMs [11]. It depends on PCM interactions that result in good NP dispersion in the polymer matrix [12].

Due to the direct methods for development of thin, uniformly thick ZnO-embedded PVA NCs films, the solution casting approach (SCA), a long-established method for developing PCMs films, was adopted. The physical properties of NCs films are significant due to their various optoelectronic applications [13].

This concept was adopted from a published research paper and involved tailoring the electrical and optical properties of the PVA matrix by adding ZnO based nanofillers [10]. Despite research work, suggesting that ZnO-integrated PVA NCs film has prospective to be used in optoelectronics, in-depth research on the application of ZnO-PVA NCs films in OSCs has not yet been available. In order to illustrate the performance effectiveness of ZnO-integrated PVA NCs films for improvement, several efforts have been made in the current study. The OSCs were assembled using epoxy resin (ER), carbon (CF), ZnO layer, and CuO layer. It was examined how addition of self-developed ZnO-PVA NCs films will affect the performance of an OSC with the internal structure [CF]/(ZnO/ER)/(CuO/ER)/CF.

2 Experimental

2.1 Developing the ZnO-PVA NCs films

The NCs films of ZnO-PVA were prepared via SCA (Fig. 1). To begin, PVA solutions were prepared by mixing it in water. PVA (4.0 ± 0.1 g) was mixed with 100 ± 0.5 mL of water to make a stock solution, repeatedly five times to prepare five solutions. To make the uniform solutions, magnetic stirrer with the speed of 450 rpm for 60 mints at 75 °C was used. Then, amounts of ZnO powder were added to the aqueous solution of PVA and solutions were shifted to ceramic mould dishes to shape the developed films. The mould dishes containing the NCs films were then placed in oven at 55–65 °C for 45–48 h.

The developed film was then easily removed from the mould dish, resulting in a flexible film. The films of PVA/ZnO NCs with various quantities of ZnO NPs were produced using the SCA approach (Table 1).

Five distinct films of ZnO-PVA NCs with varied amounts of PVA and ZnO were developed in order to generate better, and more effective films having 132×62 (mm) size and 20.0–120.0 μm in thickness are shown in Fig. 2.

3 Confirmation of developed NCs films

To confirm the obtained NC films, many analytical methods were applied. SEM was used to analyse the morphology of the films, FTIR was used to confirm the presence of functional groups in the films, XRD was used to study the diffraction patterns of the ZnO/PVA in the films, and UV–visible spectrophotometer was used to determine the absorption and bandgap of the prepared films.

3.1 Energy band gap (EBG) analysis of developed films

Using a Varian Cary 100 UV–Vis Spectrophotometer by Agilent Technologies, the films were characterised to analyse the EBG. The apparatus used in this experiment was first checked, calibrated, verified to get the error free results. In order to allow light of a certain wavelength to pass through the deposited films, the films were then kept in a chamber parallel to an UV–visible light source. Consequently, the EBG was calculated, with the presence of ZnO NPs in PVA matrix having a considerable impact on it.

3.2 Developing the OSCs by applying the developed NCs films

The OSCs were developed as a separator/salt aqueous electrolyte using copper oxide (CuO) conductive polymers and manufactured NCs film, CF, and dielectric. Optimising optical absorption and minimising loss during electron transit are key design goals of OSCs for converting and storing solar energy. By enhancing the exciton generating effect within the quantum dots, developing a wide

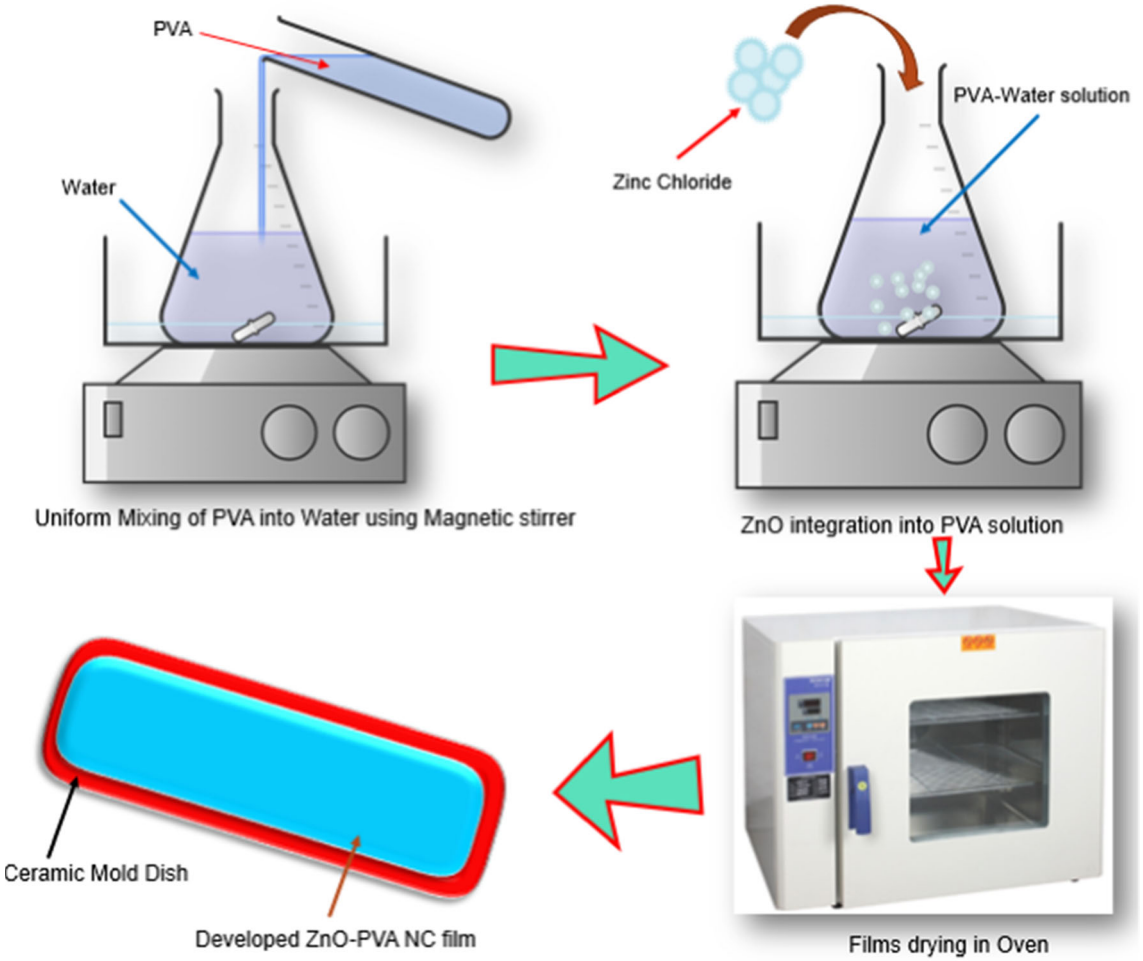

Fig. 1 ZnO-PVA NCs film synthesis via SCA

surface area, supplying certain optical effects, facilitating electron transit and collection, and producing a specific surface effect, the NCs film structure optimises the performance efficiency of OSCs.

NCs films are made using nanowires because they have fewer manufacturing defects. Therefore, a single crystal layer allows for significantly increased mobility and exceptionally efficient electron transport. Additionally, the ZnO nano-wires-based array had a significantly higher photo -current of about 58.0–78.0% than ZnO NPs sheet and 0.05–0.5 $cm^2\ s^{-1}$ diffusivity, which is several hundred times higher than titania and ZnO NPs films. The CuO co-doped polymer is applied to increase the electron concentration in polymers reinforced with CF.

The OSC structure was designed as [CF]/(ZnO/ER)/(CuO/ER)/CF (Fig. 3). In order to avoid electron flow caused by excited photons of solar radiation through surface, paper film was used as a separator in OSCs. Protons, on the other hand, can flow through the surface of the NCs film embedded layers, CuO-CF and CF. NCs films were layered on the top outer surface of OSCs and dried in a drying oven for 24 h.

3.3 Photovoltaic (electrical) studies of OSCs without NCs films

To verify the effectiveness of OSCs, a variety of electrical properties, including current–voltage (I–V), short-circuit current (J_{sc}), and open-circuit current (V_{oc}), were carefully examined. The I–V character of OSCs without NCs film was studied by analysing the I–V plot under straight solar radiations in a typical atmosphere. The J_{sc} and V_{oc} may be measured by attaching a multimeter to both portions of the OSCs using wires with alligator clips on their ends. The negative electrode (CF/ZnO/ER) was linked to the negative terminal of the multimeter, while the positive electrode (CF/CuO/ER) was attached to the positive terminal of the multimeter. The whole I–V curves were calculated using point-to-point currents and voltage. The OSCs were analysed outdoors in 32 °C direct sun heat.

Table 1 Developed NCs films

Hybrid cell	NCs film codes	Film thickness (μm)	Wt. of PVA (%)	Wt. of ZnO (%)
$ZnO_{(1)}$-$PVA_{(6)}$	NC-1	31.10	83.50	16.50
$ZnO_{(2)}$-$PVA_{(6)}$	NC-2	41.10	72.50	27.50
$ZnO_{(3)}$-$PVA_{(6)}$	NC-3	52.10	64.50	35.50
$ZnO_{(4)}$-$PVA_{(6)}$	NC-4	69.10	57.00	43.00
$ZnO_{(6)}$-$PVA_{(10)}$	NC-5	11.10	61.00	39.00

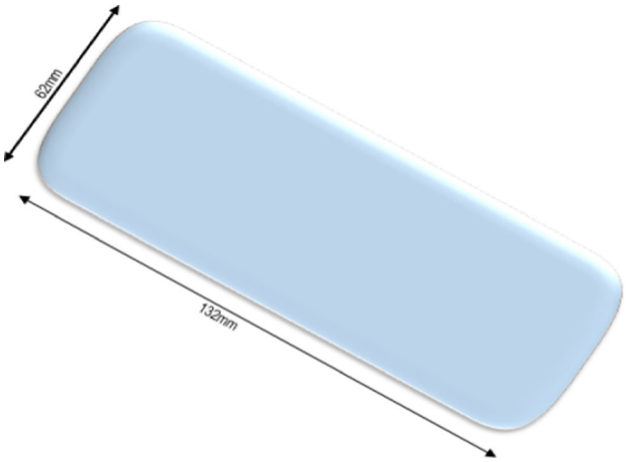

Fig. 2 ZnO-PVA NCs film (proposed shape)

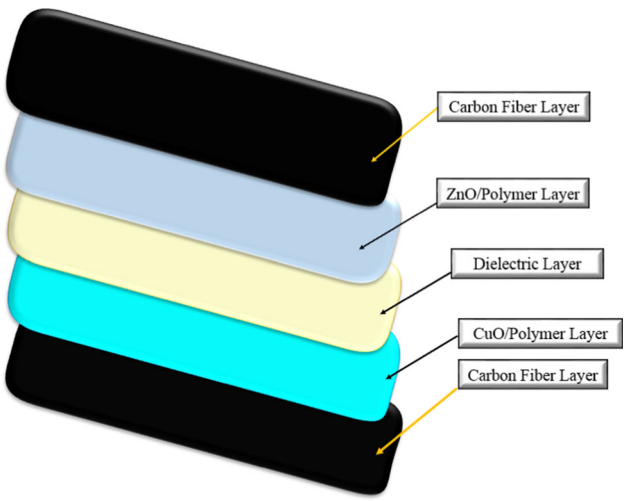

Fig. 3 Proposed architecture of prepared solar cell

3.4 Photovoltaic (electrical) studies of OSCs with NCs films

The *I–V* properties of OSCs with films integrations were studies by analysing *I–V* curves in an moderate environment under direct sun light. The V_{oc} and J_{sc} were measured by connecting a multi-meter to both sides of OSCs using wires with alligator clips attached to their terminating sides. The positive electrode (CF/CuO/ER) was connected to the positive terminal of the multi-meter, while the negative electrode (CF/ZnO/ER) was connected to the negative terminal. The entire *I–V* curves were then computed using point-to-point current and voltage measurements. The ZnO-PVA NCs film-coated OSCs were examined in direct sunlight at 32 °C.

4 Results and discussion

The prepared NC films were characterised using a variety of analytical techniques. SEM was used to perform a morphological analysis of the films; FTIR was used to confirm the presence of functional groups in the films; XRD was used to study the diffraction patterns of the ZnO/PVA in the films; and a UV–visible spectrophotometer was used to measure the absorption and bandgap of the prepared films.

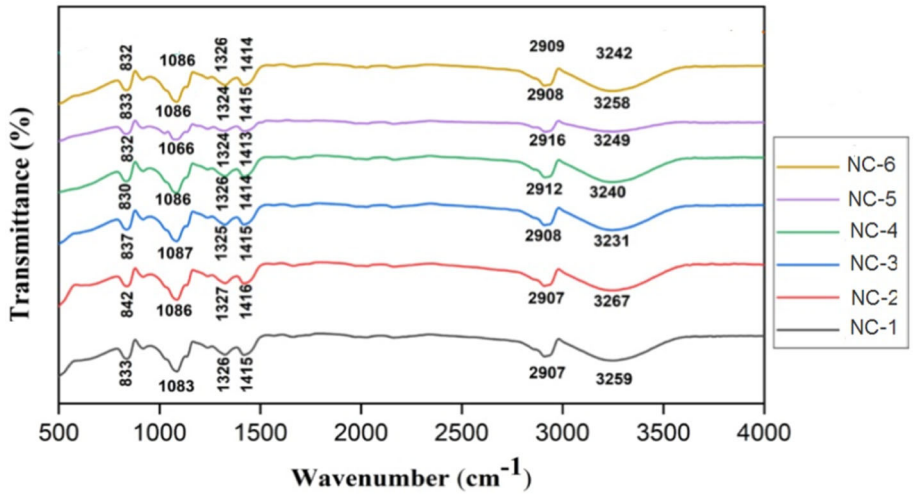

Fig. 4 Functional group analysis of all developed films

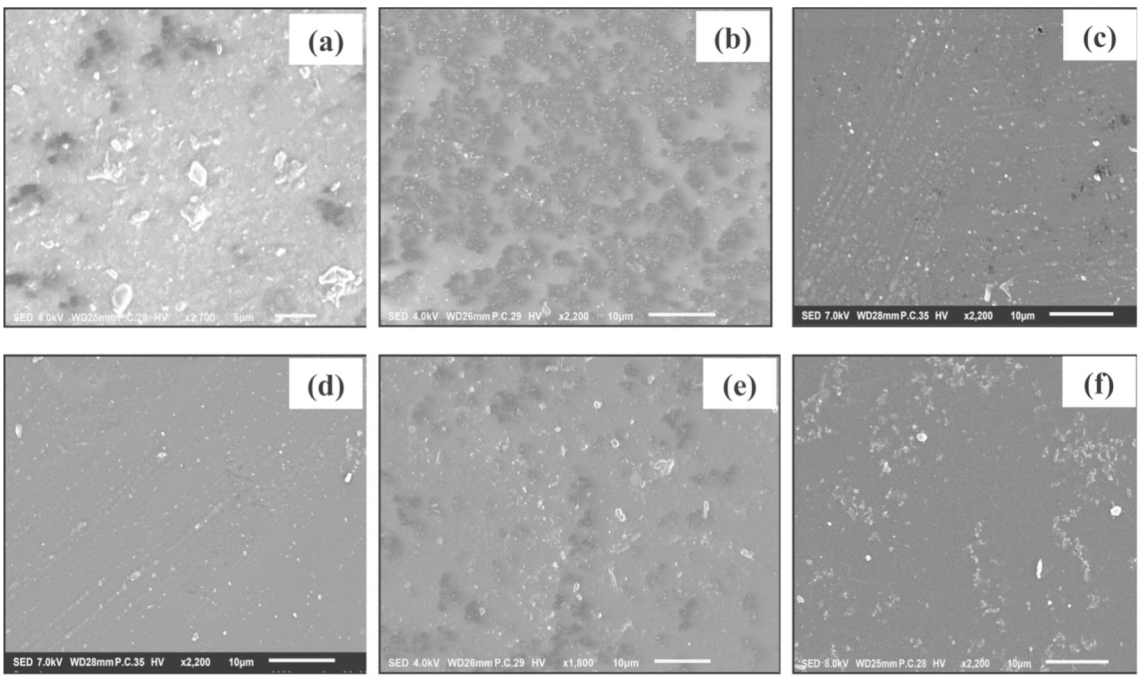

Fig. 5 SEM images of **a** NC-1, **b** NC-2, **c** NC-3, **d** NC-4, **e** NC-5, **f** NC-6

4.1 Functional group analysis

The FTIR spectra of all developed films are shown in Fig. 4. Each sample exhibits a wide absorption peak at 3259.1, 3267.2, 3231.4, 3240.4, 3249.4, 3258.7, 3242.4, 3207.1, 3259.5, and 3213.4 cm^{-1}. The bands assigned to 2907, 2908, 2912, 2916, 2908, 2909, 2917, 2909, and 2911 cm^{-1} exhibit asymmetric C–H stretching vibrations. At (1415.5, 1326.2 cm^{-1}), (1416.2, 1327.6 cm^{-1}), (1415.4, 1325.1 cm^{-1}), (1414.2, 1326.1 cm^{-1}), (1413.1, 1324 cm^{-1}), (1414.1, 1326.2 cm^{-1}), (1412.1 cm^{-1}), and (1416.11, 1325.22 cm^{-1}, there is CH_2 vibration-related absorbance (1416.1, 1320.6 cm^{-1}).

The strong band at 1082.9, 1086.1, 1087.4, 1085.9, 1065.9, 1086.1, 1086.1, 1097.1, 1085.2, and 1086.2 cm^{-1}, respectively, is connected to the C–O stretching of the PVA matrix acetyl group. The development of intermolecular hydrogen bonds between the OH groups of PVA and the ZnO surface may be the origin of the spectrum shift. PVA and ZnO are interacting, as evidenced by the change in the surrounding doping bands. Because higher ZnO concentrations lead to the agglomeration of ZnO NPs, which reduces the number of surface atoms and involvement in both the ZnO NPs and the polymer matrix, higher ZnO percentages in the PVA matrix act differently from lower ZnO percentages in the PVA matrix.

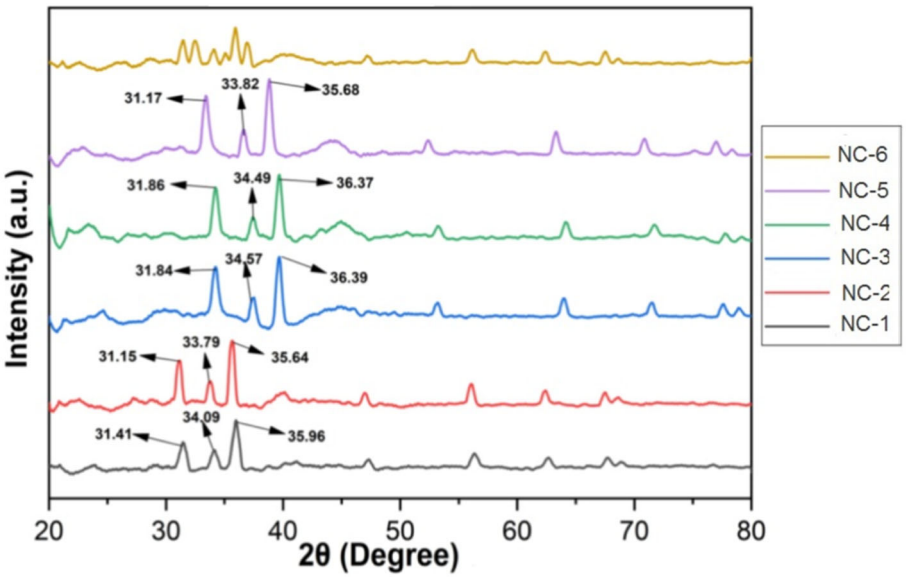

Fig. 6 XRD Pattern of prepared NC films

Table 2 Lattice parameters from XRD pattern

NC film	Miller indices (hkl)	Peak position (2θ)	FWHM (β)	D = K$\lambda/\beta\cos\theta$ (nm)	Interplanar spacing d (Å)	Lattice parameter a	Lattice parameter c	Avg. particle Size D = K$\lambda/\beta\cos\theta$ (nm)
NC-1	(100)	31.42	0.58	14.29	2.8461	3.2858	5.256	14.31
	(002)	34.08	0.57	14.23	2.6281			
	(101)	35.97	0.57	14.18	2.4960			
NC-2	(100)	31.16	0.51	16.38	2.8690	3.313	5.302	16.9
	(002)	33.78	0.50	16.78	2.6510			
	(101)	35.65	0.47	17.84	2.5169			
NC-3	(100)	31.85	0.55	15.44	2.8079	3.243	5.186	16.9
	(002)	34.569	0.439	18.78	2.5926			
	(101)	36.389	0.480	17.38	2.4668			
NC-4	(100)	31.858	0.479	16.87	2.8068	3.2408	5.1967	18.32
	(002)	34.489	0.419	19.56	2.5985			
	(101)	36.369	0.448	18.55	2.4683			
NC-5	(100)	31.169	0.518	15.82	2.8672	3.3107	5.2966	18.94
	(002)	33.819	0.368	22.12	2.6484			
	(101)	35.678	0.439	18.86	2.5144			
NC-6	(100)	31.459	0.469	17.41	2.8414	3.2809	5.5089	16.95
	(002)	32.477	0.518	15.88	2.7546			

4.2 SEM analysis

The SEM scan in Fig. 5a shows that the increased surface energy led to the development of crystal aggregates with a nanometre scale. On the other hand, the micrograph contains a lot of small particles, with an average size of 14 nm. The NC-1 film's surface morphology shows that it has a range of aggregates or pieces scattered across its top surface. The findings demonstrate that ZnO NPs have a propensity to cluster into small particles when dispersed in a PVA polymer.

A micrograph of the NC-2 film is shown in Fig. 5b, which assesses the uniform dispersion of nanoparticles inside the PVA matrix. The NC-2 showed that when the ZnO concentration increased, crystallites developed and started to grow close to the surface. Additionally, it showed that ZnO NPs were distributed uniformly, with higher ZnO concentrations leading to increased compactness and agglomeration.

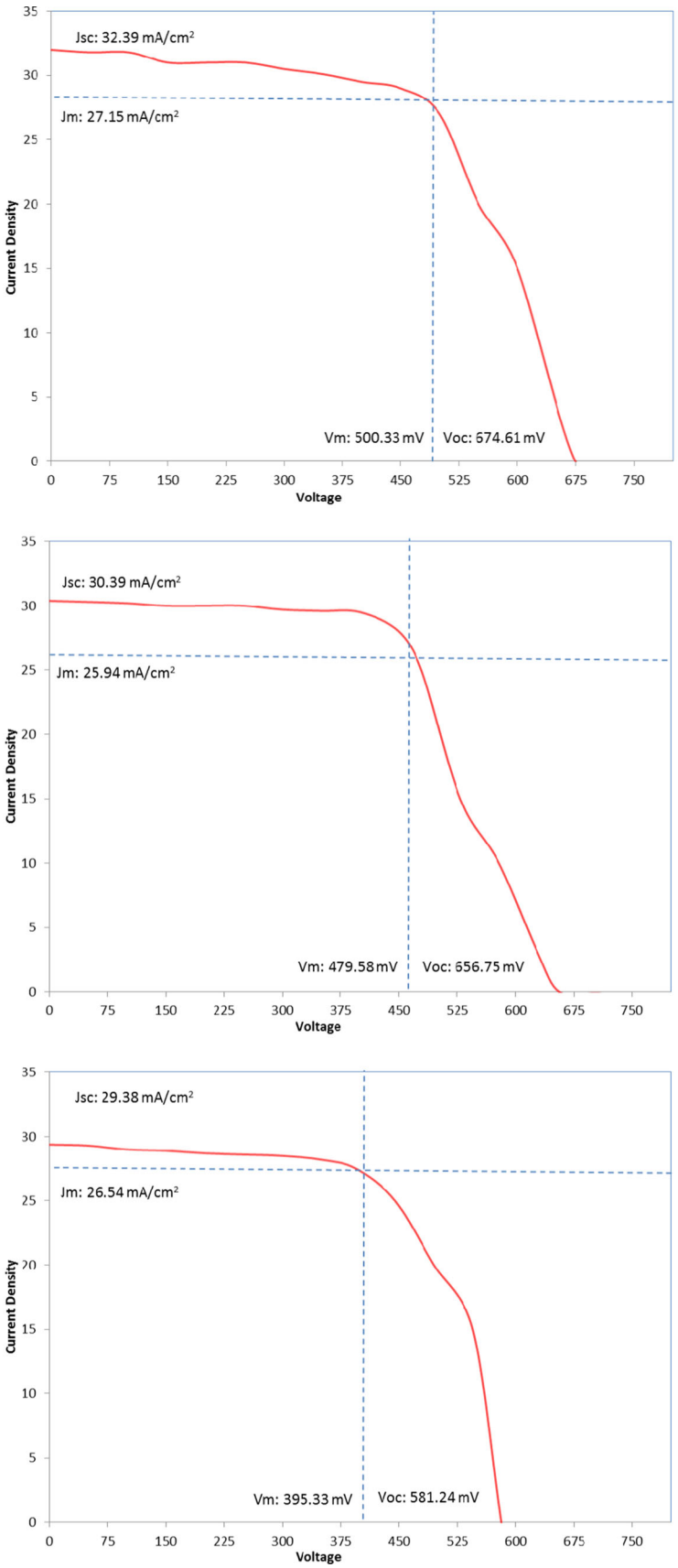

Fig. 7 **a** *J–V* curve of NC-1 film with OSCs at 32 °C (solar heat), **b** *J–V* curve of NC-2 film with OSCs at 32 °C (solar heat). **C** *J–V* curve of NC-3 film with OSCs at 32 °C (solar heat). **d** *J–V* curve of NC-4 film with OSCs at 32 °C (solar heat). **e** *J–V* curve of NC-5 film with OSCs at 32 °C (solar heat)

Fig. 7 continued

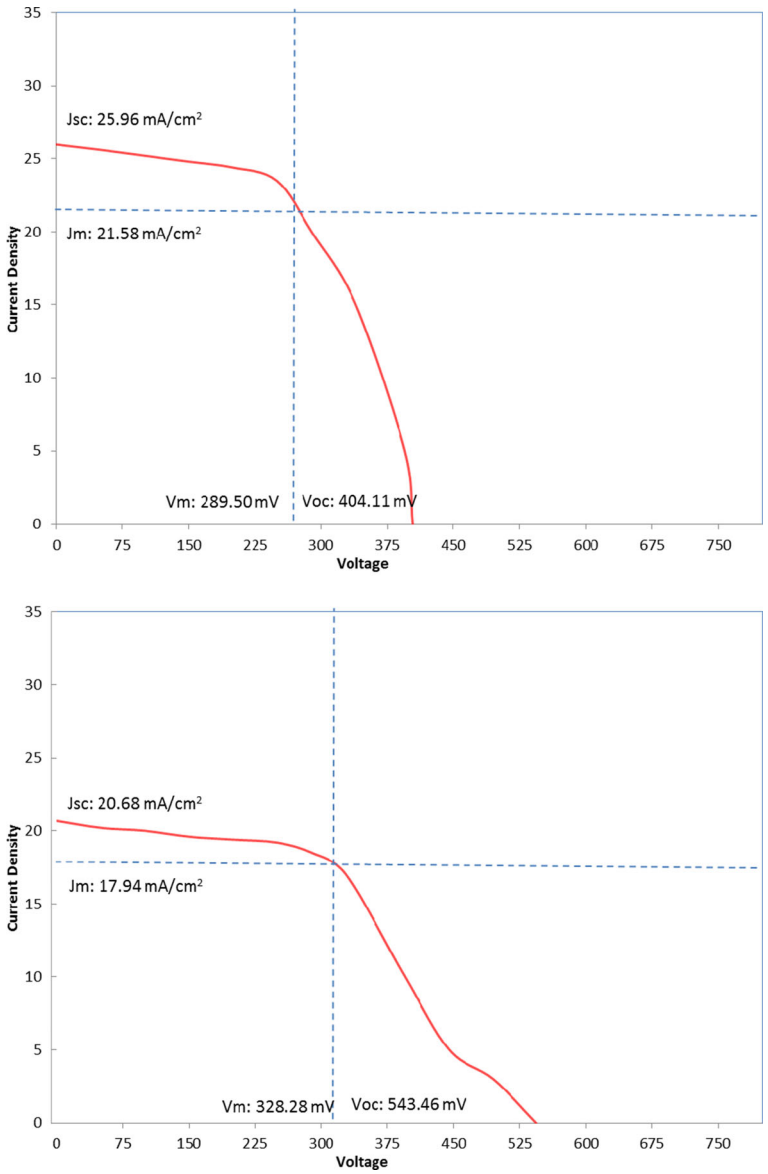

The homogeneous dispersion of nanoparticles in the PVA matrix is examined in the SEM image of NC-3 film in Fig. 5c. The top surface of developed NCs films is covered in many clumps or pieces that are dispersed randomly. It is important to emphasise that erratic ZnO nanoparticles have been produced, ranging in size from 15 to 18 nm.

An evenly processed smooth PVA matrix with flaked-shaped ZnO particles dispersed over the surface is shown in Fig. 5d. It is important to note that erratic ZnO nanoparticles have been produced, ranging in size from 16 to 19 nm.

Figure 5e shows a SEM image of a smooth, uniformly processed PVA matrix with large ZnO NPs and an irregular shape. The image demonstrates an increase in compactness when ZnO NPS concentration in the polymer matrix rises.

ZnO particles are shown in Fig. 5f as they aggregate from many starting crystallites of different sizes and shapes in NC-6. As the ZnO concentration rises, compactness appears in various locations, suggesting that the sample is becoming more crystalline.

4.3 XRD analysis

Figure 6 displays the XRD patterns of all samples with a comparable high peak of 2 = 35.961, 35.641, 36.392, 36.369, 35.681, 35.911, 35.662, 36.471, and 36.781. The relevant diffraction peaks were matched to the PVA diffraction peak and the PDF database of the conventional hexagonal ZnO wurtzite crystal structure (JCPDS 36-1451). These diffraction peaks proved that ZnO/PVA NCs had formed. Six samples of PVA/ZnO NCs film's crystallite size were determined using the Debye–Scherrer formula, as shown in Table 2. While excessive doping of ZnO NPs reduces crystallinity due to crystalline size variability and aggregation formation,

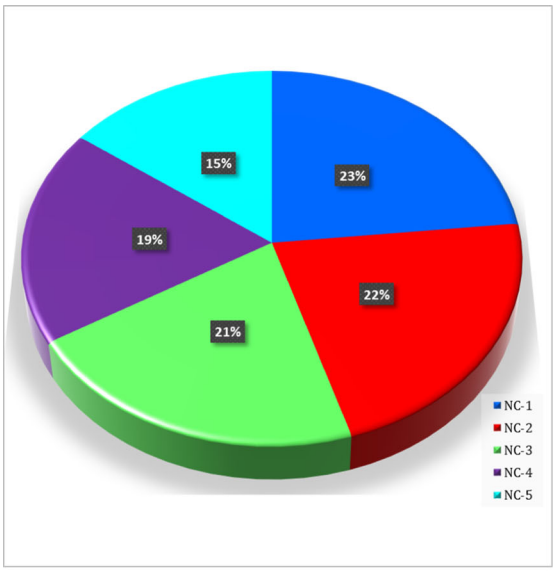

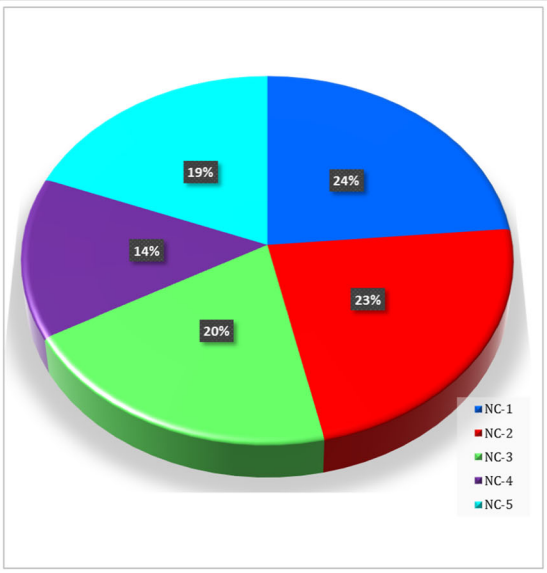

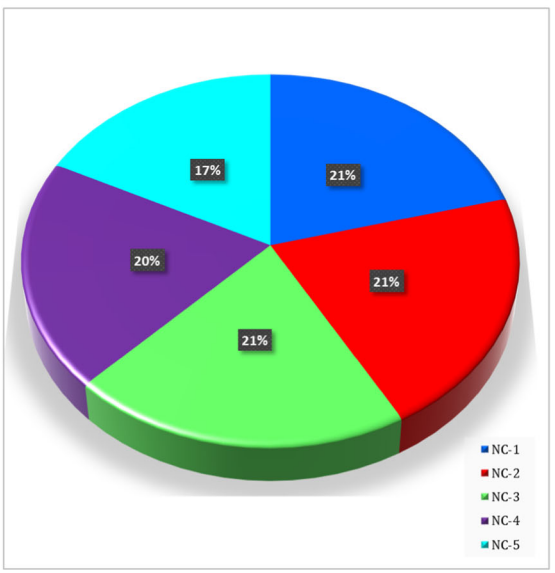

Fig. 8 **a** Open-circuit density of prepared films in designed OSCs, **b** open-circuit voltage of prepared films in designed OSCs, **c** fill factor of prepared films in designed OSCs, **d** EBG of prepared films in designed OSCs

Fig. 8 continued

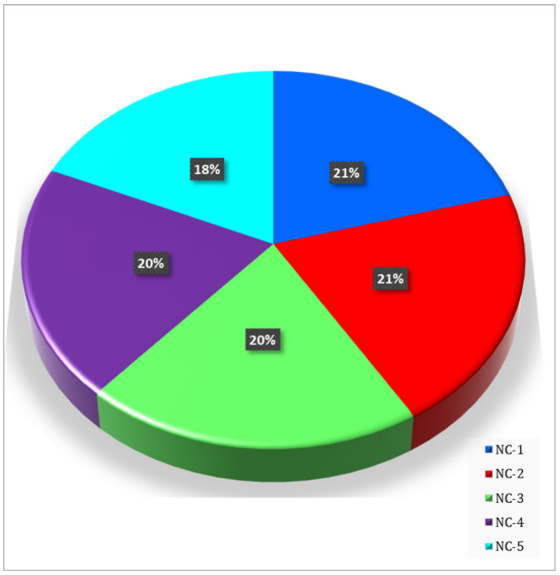

Fig. 9 Performance efficiency parameters of prepared films in designed OSCs

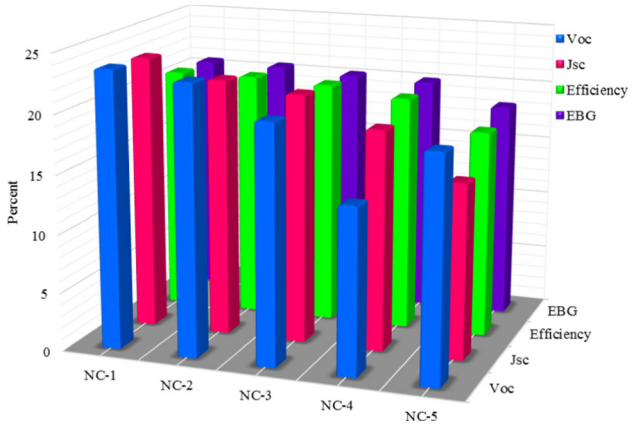

doping ZnO nanoparticles enhances their crystallinity. Particle size expansion is indicated by contractions in peak breadth and peak sharpness. The ZnO NPs matrix influence of PVA has increased the strain in the NCs films.

4.4 Performance efficiency investigation

In order to assess how the performance efficiency of the OSCs changed at 32 °C under solar energy, five different films of ZnO-PVA NCs (Fig. 7a–e) were evaluated independently with the OSCs. According to the outcomes of the generated NCs films, improving organic solar performance results in lower performance when ZnO NP amount is increased. A smaller band gap for the films might potentially be the outcome of this. The lowest current density performance indicates that a greater amount of ZnO creates a wire-like film where current flow is restricted, resulting in less energy development.

Each of the developed NCs films was evaluated separately with OSCs in direct sunlight in accordance with the performance of thin films of ZnO-PVA with varied compositions. The efficiencies attained by the OSCs combined with ZnO-PVA NCs films are shown in Table 2. The highest efficiency of NC-1 is 13.57%, while the lowest efficiency of NC-6 is 5.88%. Several variables, including J_{sc}, fill factor (FF), and V_{oc}, have an impact on efficiency. The proportion of variables affecting OSC efficiency is shown in Fig. 8a–d. As FF decreases, OSC efficiency decreases. Efficiency was lost when the optical direct bandgap shrank with increasing ZnO content in the polymer matrix. The efficiency of OSCs is also impacted by the thickness of NCs films,Fig 9 with a decrease in efficiency as the thickness of NCs films increases.

4.5 Performance efficiency evaluation of OSCs using developed films

Under 32 °C solar heat, the optimised films with varying wt% of PVA and ZnO within an OSCs, were studied. Open-circuit voltage (V_{oc}), energy conversation efficiency (gec), and current density (J_{sc}) are the key parameters for the thin-film with OSCs that have been described.

With a 4.16 eV EBG, or extraordinarily wide band gap, crystalline ZnO can absorb solar energy. Table 3 demonstrates that the NCs film with a composition of 16.50% ZnO and 84.50% PVA is the best film for increasing OSC efficiency by almost 4.0%. Without NCs film, OSC had a 10.08% efficiency.

Performance efficiency is maximised by using thin coatings, proving that they perform somewhat similarly to *n*-type semiconductors. The mobile electrons receive energy from the photo electrode-absorbing NCs film when the sun rays strike it, and an electron with the best energy goes through the OSCs layer, leaving space open for another electron. The electrons are taken in and converted into energy by the top ZnO/ER electrode. These electrons complete the circuit by interacting with additional electron vacancies at the bottom CuO/ER electrode.

5 Conclusion

All films of ZnO-PVA NCs in this study were effectively developed using the solution casting method. ZnO and PVA NPs are combined in a weight-per-weight ratio in each film. To ascertain the impact of the ZnO-PVA NCs layer on OSCs efficiency, these films were examined utilising OSCs. The NC-1 optimised sample has an efficiency of 13.57%, which is higher than NC-5 efficiency of 5.88%. J_{sc}, FF, and V_{oc} are the variables that affect how effective OSCs are.

The effectiveness of OSCs decreases along with the FF. Efficiency was lost as the amount of ZnO in the polymer matrix rose because the optical direct EBG decreased. The performance of OSCs is also impacted by the produced NCs film's thickness, with increasing NCs film thickness resulting in a decrease in efficiency. The film with ZnO (16.50%) and PVA (84.50%) showed the highest efficiency compared to the other samples.

The highest efficiency of 13.57% was found, emphasising the possibility of using NCs films in photovoltaic investigations to boost OSC efficacy. Finding the ideal drying time is necessary to produce a NCs thin film with superior physiochemical characteristics. In order to boost their attractiveness in terms of increased efficiency, future research should concentrate on enhancing the deposition quality of ZnO-PVA NCs layer on OSCs.

Declarations

Conflict of interest All authors declared that they have no conflict of interest for this research work.

Data availability statement No data associated in the manuscript.

References

1. Khan, S. A., et al. (2021). "The impact of film thickness on the properties of ZnO/PVA nanocomposite film." **8**(7): 075002.
2. M. Mohammed et al., Enhancing the structural, optical, electrical, properties and photocatalytic applications of ZnO/PMMA nanocomposite membranes: towards multifunctional membranes. J. Mater. Sci. Mater. Electron. **33**, 1–26 (2021)
3. E. Ferrone et al., ZnO nanostructures and electrospun ZnO-polymeric hybrid nanomaterials in biomedical, health, and sustainability applications. Nanomaterials (Basel) **9**(10), 1449 (2019)
4. Manikandan, P. N., et al.: Self-powered polymer–metal oxide hybrid solar cell for non-enzymatic potentiometric sensing of bilirubin. **2**(2), e10031 (2019)
5. S. Ramadan, *Deposition of zinc oxide transition metal doped and in polymer composites* (University of Manchester, Manchester, 2018)
6. L. Lou et al., Functional nanofibers and their applications. Nanofibers **59**(13), 5439–5455 (2020)
7. K.W. Leong et al., Rechargeable Zn-air batteries: recent trends and future perspectives. Renew. Sustain. Energy Rev. **154**, 111771 (2022)
8. R. Srivastava, *Electrospinning of Patterned and 3D Nanofibers Electrospun Nanofibers* (Elsevier, New York, 2017), pp.399–447
9. A. Sangwan et al., *Nanocomposites: Preparation, Characterization, and Applications. Nanotechnology: Principles and Applications* (Routledge, London, 2021), pp.201–247
10. S.A. Khan et al., Performance investigation of ZnO/PVA nanocomposite film for organic solar cell. Mater. Today Proc. **47**, 2615–2621 (2021)
11. V.G. Sreevalsa, A.M. Sajimol, S. Jayalekshmi, Characterization of transparent PVA/amino acid complex capped ZnO nano composite films. Int. J. Plast. Technol. **15**(1), 10–18 (2011)
12. M. Wu, G. Zhang, H. Yang, X. Liu, M. Dubois, M.A. Gauthier, S. Sun, Aqueous Zn-based rechargeable batteries: Recent progress and future perspectives. InfoMat 4(5), e12265 (2022)
13. Srivastava, R.J.E.N.: Indian Institute of Technology Delhi, New Delhi, India, pp. 399 (2016)